1

"Critical States of Soil and Geotechnical Centrifuge Tests"

Geotechnical Society 2016

Andrew N. Schofield, Cambridge University Engineering Department

2

Coulomb's (1773) design strength

$$\tau = c + \sigma' \tan \phi_d$$

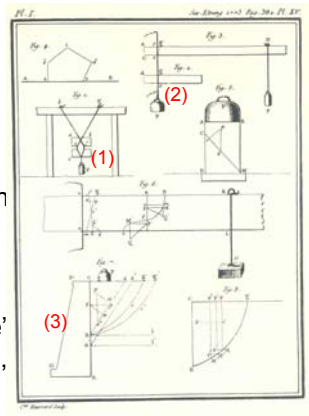

- Coulomb shows two tests to find cohesion for rock and brick. Data in tension (1) were lower than shear (2), so a tension test gave a safe cohesion value to use in design.
- He never tested soil; he took "nulle' cohesion $\phi = \phi_d$, c = 0 for disturbed, rammed earth (3).

3

Terzaghi (1936) wrote that there is a "Fundamental fallacy…" as he measured lateral earth pressures different from the computed plane limiting stress fields, solving 3 equations in 3 unknowns (σ'_x, τ_{xy}, σ'_y). For soil with Tresca's constant cohesion c′ the equations to be solved are 1 constitutive equation + 2 equilibrium equations

$(1/4)(\sigma'_x - \sigma'_y)^2 + \tau_{xy}^2 = c'^2$.

$(\delta\sigma'_x / \delta x) + (\delta\tau_{xy} / \delta y) = 0$

$(\delta\tau_{xy} / \delta x) + (\delta\sigma'_y / \delta y) = \gamma$

The equilibrium equations are correct, hence Terzaghi's "Fallacy" must have originated in a fallacious constitutive equation.

Neither the Mohr-Coulomb nor Tresca equations include a strain variable; but measured lateral earth pressures depend on strain.

When constitutive equations that attribute constant limiting-stress to every slip plane are replaced by alternative plastic-stability and plastic-work-dissipation equations we derive the Cam clay model.

4

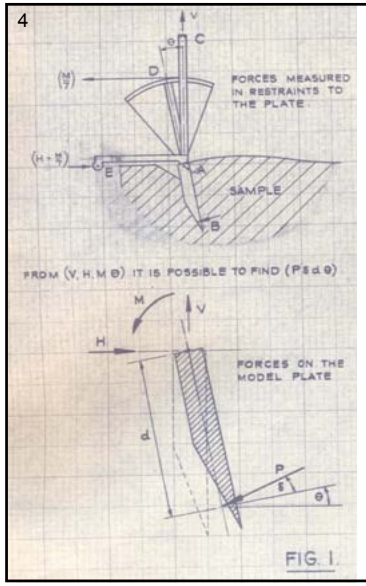

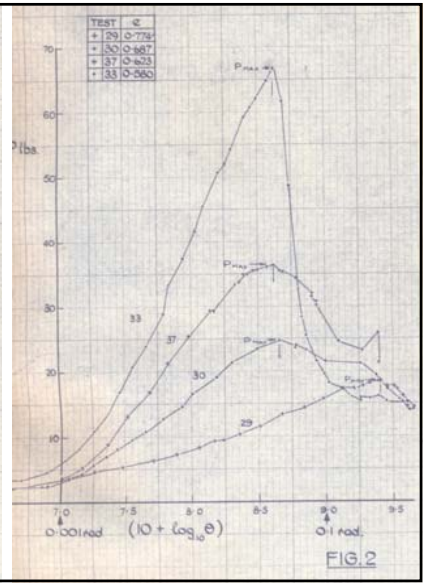

5

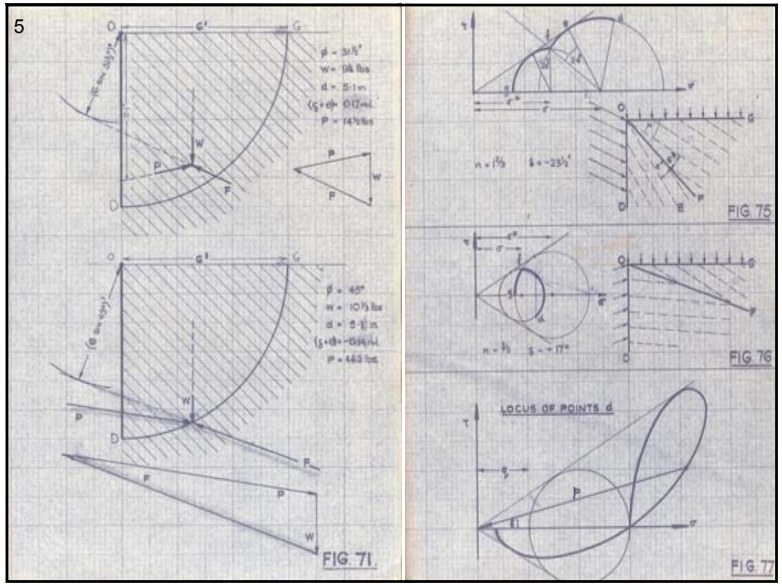

6

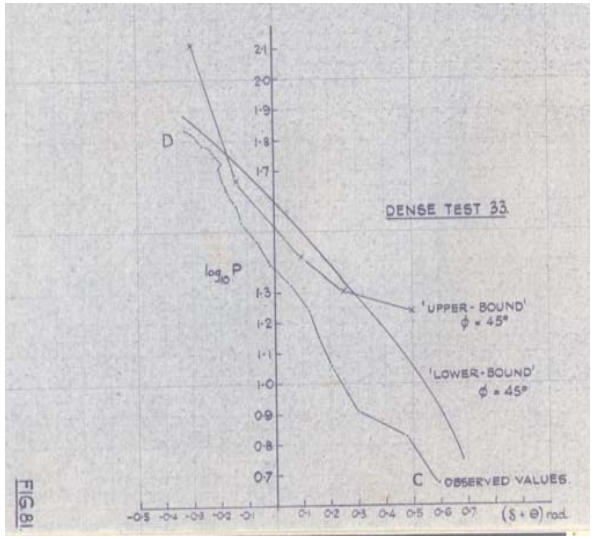

7

hinge

X ray through a plane failure (James 1965)

Plat e

A plate rotates about hinge at top left. Dense sand to right of toe the toe shears and dilates. A failure zone of loose sand (dark radiograph) develops in front of the toe. The lateral passive earth pressure force increases as the plate rotates. The toe moves up, initiating shearing and dilation in a new upper failure zone, that finally breaks out of the dense sand surface at the top right. By then the initial "failure zone" is inactive; what we see is "progressive failure".

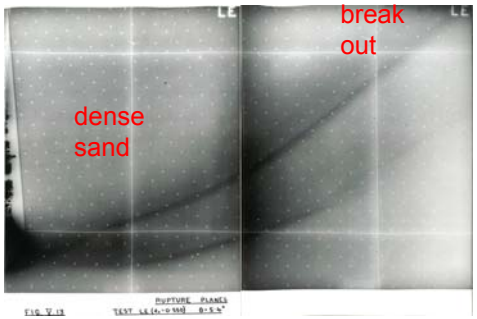

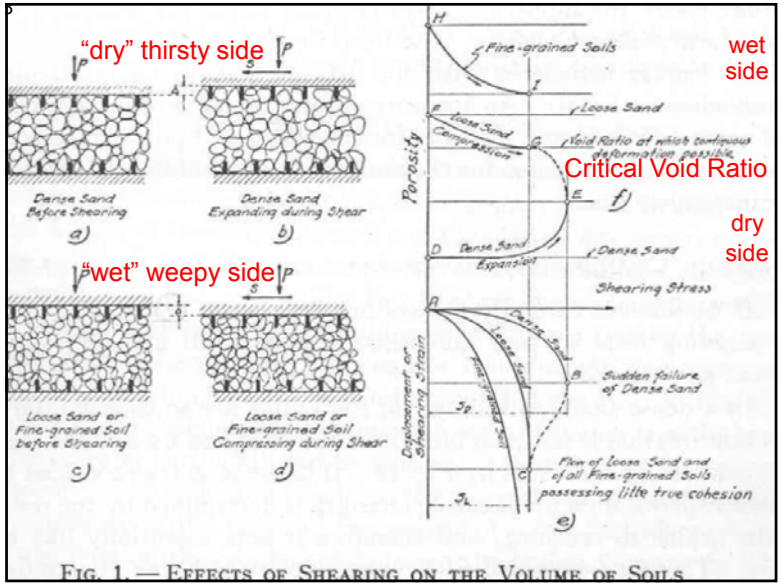

FIG. 1. — EFFECTS OF SHEARING ON THE VOLUME OF SOILS

9

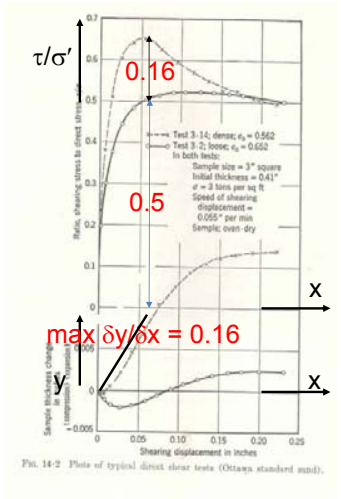

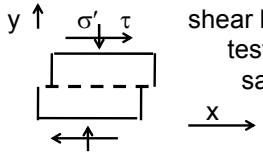

shear box test of sand

Taylor's "interlocking" equation $\tau\delta x = \sigma'\delta y + \mu\,\sigma'\,\delta x$ includes a Work-Dissipated component:- $\mu\,\sigma'\,\delta x = (\tau\delta x - \sigma'\delta y)$. In steady slip a friction coefficient $\mu = 0.5$ applies. The peak stress ratio $\tau/\sigma' = 0.66$ here is the sum of (steady friction) $\mu = 0.5$, plus (interlocking) $\delta y/\delta x = 0.16$.

"Interlocking and Dissipation"; Taylor's (1948) data interpretation

10

Taylor's MIT shear box tests (interlocking work)

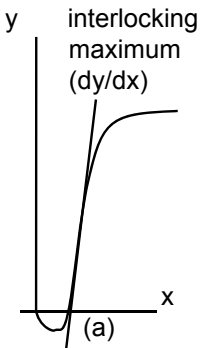

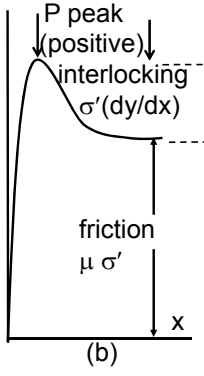

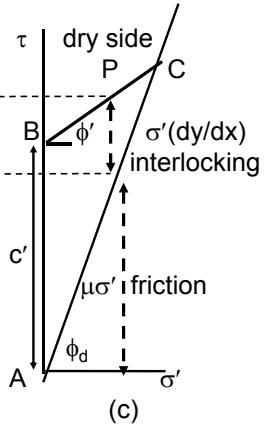

Taylor's interlocking strength equation $\tau dx = \mu\sigma' dx + \sigma' dy$

strength = friction + interlocking

Peak drained strength at P; see Schofield (2006) Géotechnique

11

a) In a loose aggregate p′ is mean effective pressure; dε is shear distortion

b) Hourglass sand at rest stands as a plastic solid

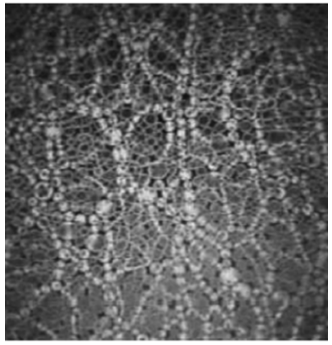

c) In Allersma's photo elastic image every bright grain stores energy. If p′ increases the grains get more bright. If dε increases more struts will buckle. A function M p′ dε gives work dissipation

12

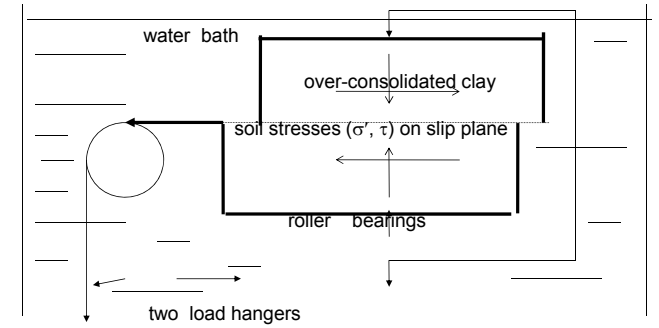

(1) shear force, τ, displacement dx (2) normal force, σ′, dilation dy

Hvorslev's drained shear box tests caused thin slip failure

13

Hvorslev used Terzaghi's shear box to prepare and test clay with test paths from D to H to E (normal consolidation), from E to C to B (swelling) from B to F (slow increase of shear stress to peak-strength). He divided stresses by σ'_e in order to normalise pressures to line FAH as if all peaks were at w.

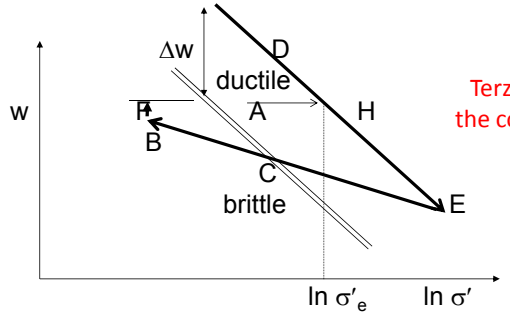

Terzaghi/Hvorslev; the cohesion blunder

14

Shear box tests of clay

Hvorslev's plotted data of clay compression and swelling, with solid lines before peak strength and dashed lines at slip, ➔

All peak shear strengths are quite close to and only just above a line with zero cohesion and fully softened friction ϕ_d

Data for σ'/σ'_e values in a range $0 < \sigma'/\sigma'_e < 0.6$, but not for $0.6 < \sigma'/\sigma'_e$ ➔ Wet side of CS; no slip.

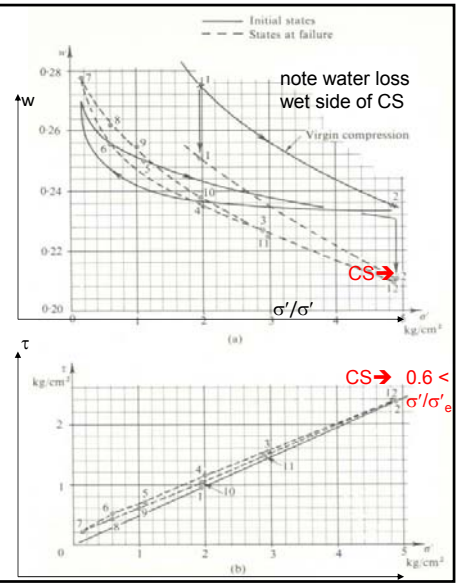

15

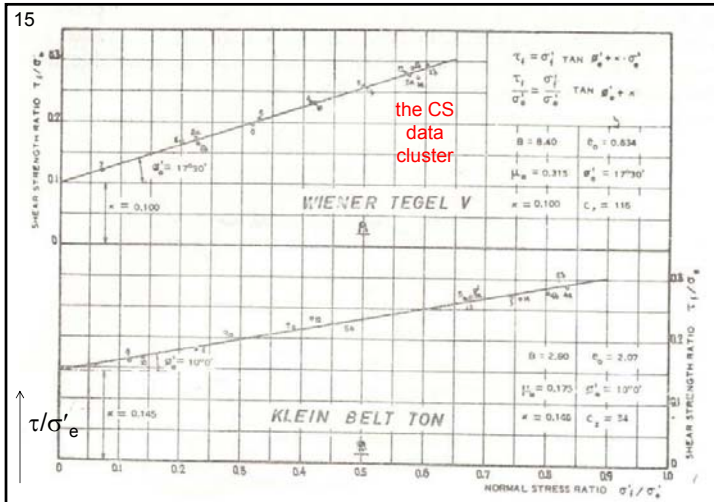

σ'/σ'_e Hvorslev's peak strengths σ' normalised by σ'_e

16

From principal stresses σ'_1, $\sigma'_2 = \sigma'_3$ we derive two state parameters; spherical stress $p' = \{(\sigma'_1 + 2\sigma'_2)/3\}$, and deviator stress $q = (\sigma'_1 - \sigma'_2)$.

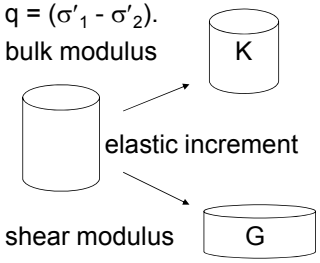

A unit volume of solids in a grain-aggregate occupies v=(1+e). K is spherical effective stress p′ over volumetric strain; G is deviator stress over deviator strain.

Elastic media shear with v=const.; an increment in spherical stress $\delta p'$ causes volumetric strain decrement δv with no shear distortion because in elastic media $+/-\delta q$ anti clock and clockwise shear stress increments cause $+/-\delta\varepsilon$ shear strain increments.

Grain aggregates are plastic; $+/- \delta\varepsilon$ causes a dense aggregate to dilate and a loose aggregate to contract.

17 a) define deviator stress $q = (\sigma_a - \sigma_r)$, and $p' = (\sigma_a + 2\sigma_r)/3 - u$, with σ_a axial pressure, and $\sigma_a = \sigma_r + (\sigma_a - \sigma_r) = \sigma_r + q$.

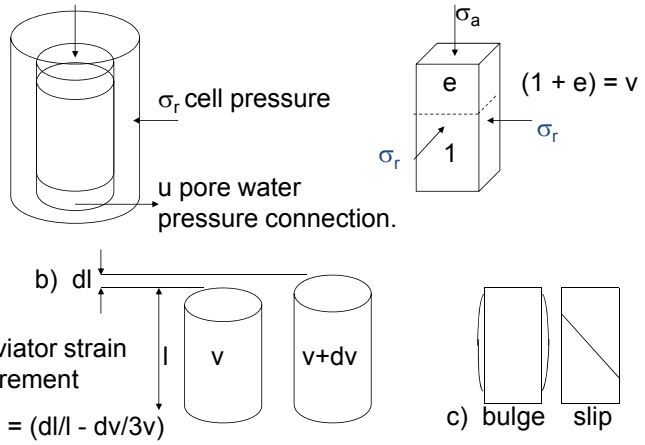

Soil States in Triaxial Test; plot data as state points (p′, q, v)

18

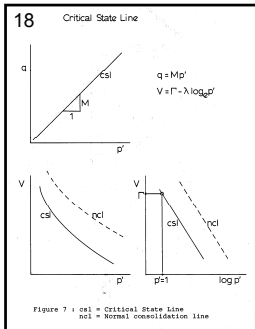

Roscoe, Schofield, & Wroth's (1958) (p′, q, v) test-data paths approach a Critical States line

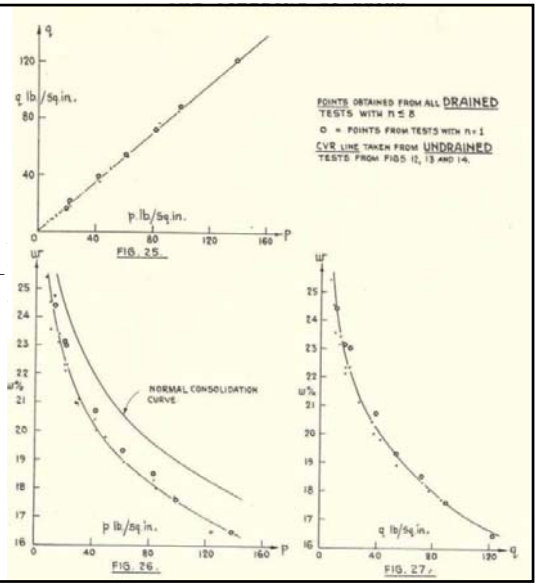

19 Plasticity Index based on 80gm and 240gm fall cone tests

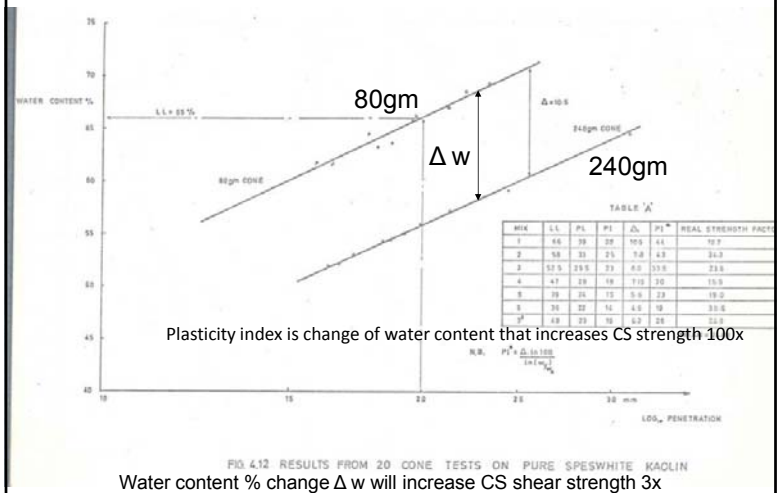

Plasticity index is change of water content that increases CS strength 100x

Water content % change Δ w will increase CS shear strength 3x

20

Ductility and continuity in soil mechanics

- A paste of soil saturated with water is plastic, (from the Greek word πλασσειν plassein to mould, as in moulding pottery from clay).
- An aggregate of separate hard grains in a critical state will behave as a ductile plastic continuous material.
- Plastic design leads us to select construction materials and methods; soil, if over compacted to high peak strength, is not plastic and ductile

21

Strains by the associated plastic flow rule

In plastic flow, as a body yields under combined stresses $\sigma_i\ \sigma_j$ with strain increments $\delta\varepsilon_i^p\ \delta\varepsilon_j^p$, the flow vector is normal to the yield locus at $(\sigma_i\ \sigma_j)$. For stability the product of any stress increment vector $(\delta\sigma_i\ \delta\sigma_j)$ and the plastic strain rate flow vector may not be negative; $\delta\sigma_i\ \delta\varepsilon_i^p + \delta\sigma_j\ \delta\varepsilon_j^p > 0$.

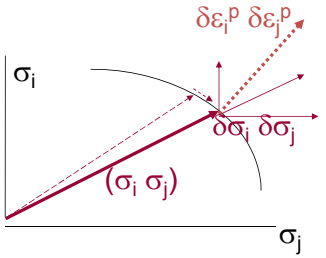

22

Construction without plastic ductility

Ductility can save life. The 1995 Oklahoma Federal Centre bomb damage showed how a lack of continuity and ductility will cause a risk of brittle failure.

23

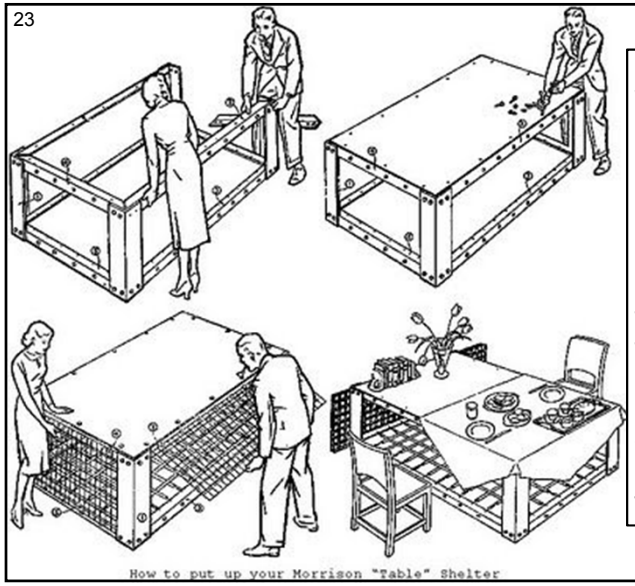

"Morrison" WW2 mild steel bomb shelter had PLASTIC DESIGN by Prof John Baker on the basis of the work dissipated in rotations of "plastic hinges" at failure.

24

Plastic design of steel frame structures, Baker (1948)

- A WW II 250kg bomb burst near a Falmouth house. As it collapsed the 20 lb/sq.ft upper-floor load fell 9 ft on the bomb shelter, A mother and 3 children survived, asleep in the shelter.
- Space inside any structure is made more safe by designing full plastic strength at floor to wall connections (contrast photo with structural failures of Oklahoma Federal Center and New York Twin Towers).

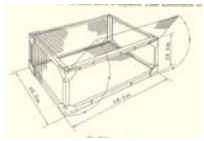

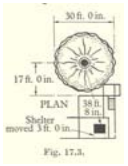

25

Derivation of original Cam-clay (1963) $q/Mp'=1-\ln(p'/p'_c)$

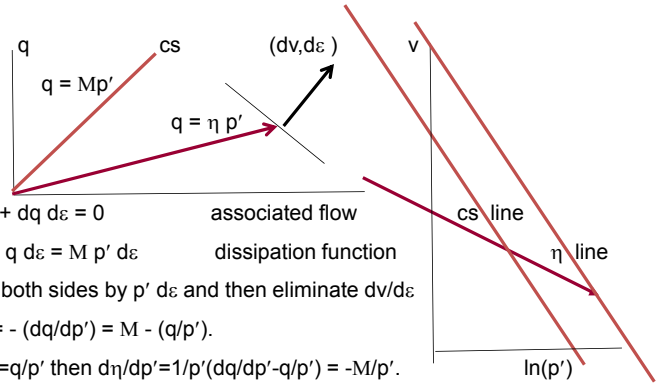

$dp'\,dv + dq\,d\varepsilon = 0$ associated flow

$p'\,dv + q\,d\varepsilon = M\,p'\,d\varepsilon$ dissipation function

Divide both sides by $p'\,d\varepsilon$ and then eliminate $dv/d\varepsilon$

$dv/d\varepsilon = -(dq/dp') = M - (q/p')$.

With $\eta=q/p'$ then $d\eta/dp'=1/p'(dq/dp'-q/p') = -M/p'$.

Hence $\ln p'\,d\eta = -M dp'/p'$. When integrated this gives $\eta/M=1-\ln(p'/p'_c)$.

26

Thurairajah's (1961) analysis

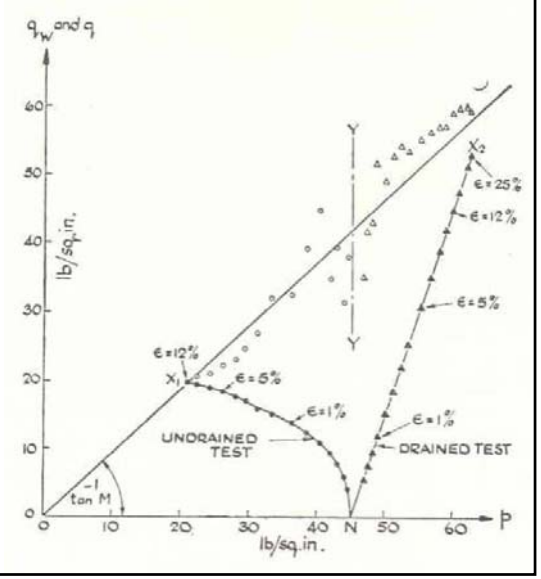

27

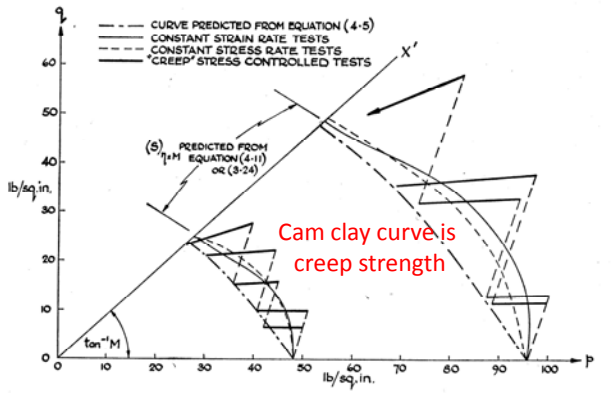

Fig. 18. Predicted and observed stress paths for undrained tests on Cambridge Gault Clay. (Stress controlled test data, by W. J. Thompson (1962))

Cam clay curve is creep strength

Thompson (1962) creep data

28

London clay "cut-face stand-up" model test

Henkel (1956) shows moist slip-surfaces in stiff fissured 'lubricated-block" London clay rubble behind an old retaining wall. Skempton suggested that clay strength is time dependent. An alternative is for stand-up to involve diffusive swelling to Critical-state failure as in this model of Bradwell cut stand-up time (i.e. Lyndon & Schofield 1972, not Skempton & La Rochelle1965)

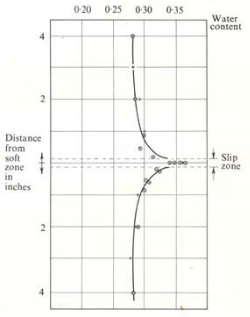

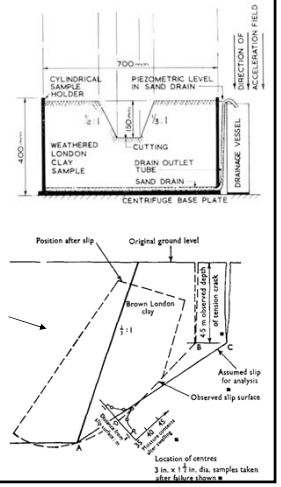

29

Bazalgette's sewer system. Image: N. Barton, "Lost Rivers of London" (Modified)

30

A backdrop will reduce sewer flow rate, but will cause deep trench-heading damage

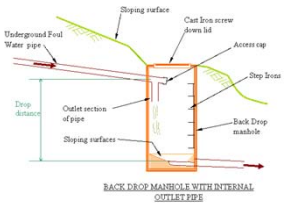

31

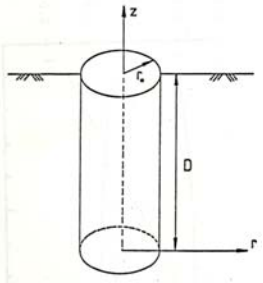

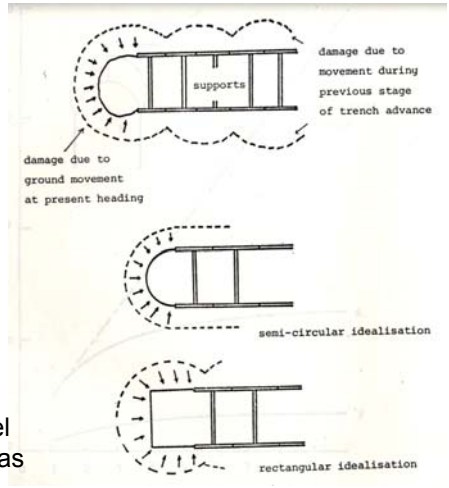

Kusakabe's model tests for British Gas

32

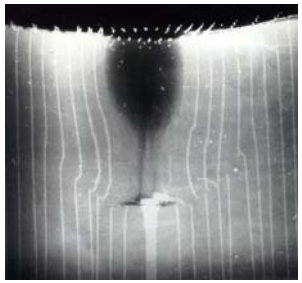

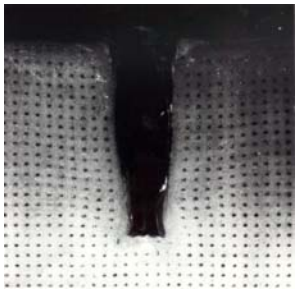

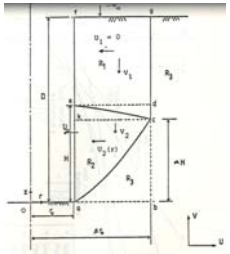

1980 centrifuge-model test by PhD research student Osamu Kusakabe (now Professor, Tokyo Institute of Technology) showed axisymmetric circular shaft failure mechanism.

33

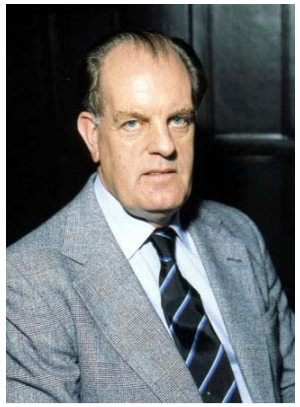

Sir Denis Rooke
1924-2008

Sir Edwin Chadwick
1800-1890